Three-dimensional graphene enhanced heat conduction of porous crystals

Citation: Yang, Sungwoo et al. "Three-Dimensional Graphene Enhanced Heat Conduction of Porous Crystals." Journal of Porous Materials 23.6 (2016): 1647–1652.

As Published: http://dx.doi.org/10.1007/s10934-016-0225-9

Publisher: Springer US

Persistent URL: http://hdl.handle.net/1721.1/105175

Version: Author's final manuscript: final author's manuscript post peer review, without publisher's formatting or copy editing

Three-Dimensional Graphene Enhanced Heat Conduction of Porous Crystals

Sungwoo Yang, Xiaopeng Huang, Gang Chen and Evelyn N. Wang*

Department of Mechanical Engineering, Massachusetts Institute of Technology, 77 Massachusetts Ave, Cambridge, MA 02139

Corresponding Author

* To whom correspondence should be addressed E-mail: enwang@mit.edu

Dr. Evelyn N. Wang
Email: enwang@mit.edu
Tel: (617) 324-3311
Fax: (617)258-9346

KEYWORDS: GRAPHENE FOAM, THERMAL CONDUCTIVITY, POROUS COMPOSITE, ZEOLITE, METAL ORGANIC FRAMEWORKS, ADSORPTION, GAS SEPARATION, HYDROGEN STORAGE

Supporting Information Available

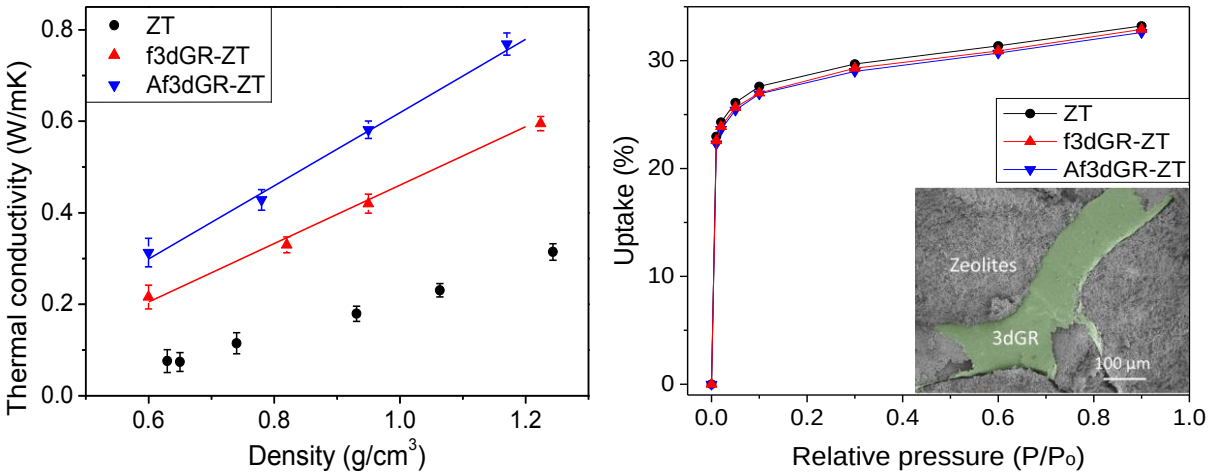

* Zeolite (ZT), Three-dimensional graphene (3dGR), Functionalized 3dGR (f3dGR), Annealed f3dGR (Af3dGR)

ABSTRACT: We present functionalized three-dimensional graphene as a promising thermal additive to increase the effective thermal conductivity of porous crystal adsorbents. Due to the percolation and high porosity of three-dimensional graphene, the thermal conductivity of the adsorbent-graphene composite was enhanced up to 500% with a minimal reduction in adsorption capacity of approximately 2%. The functionalization demonstrated to be an effective way to implement a hydrophobic carbon network with hydrophilic porous crystals. The functionalized three-dimensional graphene can be applicable to numerous types of porous crystals including zeolites and metal organic frameworks to overcome their intrinsic low thermal conductivity. This work provides insights for the development of binders for enhanced thermal performance of porous materials in various adsorption systems.

INTRODUCTION

Modern porous crystals, such as zeolites and metal-organic frameworks (MOFs), have great potential in various applications such as gas storage, climate control, heat-pumps, chillers, and adsorptive thermal storage.[1-6] These applications, however, require the incorporation of high thermal conductivity materials to effectively dissipate the heat generated during the adsorption process. The high

temperatures, resulting from the low crystal thermal conductivity due to their open pore structure and high total pore volumes, often lead to a reduction in the adsorption capacity as well as the reliability of the adsorbents.[7-11]

Important criteria for effective thermal additives for porous crystal absorbents include percolated structure, high porosity, and low temperature integration with adsorbents. Conventional one- or two-dimensional thermal additives such as carbon nanotubes, nanowires, graphene, and graphite, can increase the effective thermal conductivity of composite if their dispersion is suitable. However, many microporous adsorbents such as zeolites and MOFs have open pore structures and high total pore volumes, which present unique challenges in additive percolation. For example, our previous study demonstrated that the thermal conductivity improvement (~ 25%) achieved by adding one- or two-dimensional thermal additives (~ 3 wt%) was limited by the high interfacial thermal resistance between adjacent non-percolated graphene flakes.[12] On the other hand, by adding a sufficient amount of graphite, noticeable improvements in thermal conductivity of microporous adsorbent materials have been made, but at the cost of high additive fractions (>10 wt%) that compromise the total adsorption capacity.[13-15] Ideally, a small volume fraction of three-dimensional thermal additives with high thermal conductivity can be mixed with the bulk adsorbent material to minimize the reduction of adsorption capacity. For example, percolated graphene films have been coated on porous ceramic by chemical vapor deposition (CVD), demonstrating considerable improvement in thermal conductivity (4.17 W/mK, 366% enhancement) with low thermal additive fractions.[16, 17] However, this process requires high temperatures, which restricts the types of microporous adsorbents that can be used such as MOFs.[9]

In this work, we present three-dimensional graphene (3dGR) as a thermal additive to enhance the effective thermal conductivity of porous crystal composites. 3dGR is a few layer graphene foam

synthesized by CVD. While its thermal conductivity has been characterized[18], the integration of porous crystals have not been studied yet. The percolated structure of 3dGR enables efficient thermal conduction through connected graphene flakes, even at low volume and weight fractions, thereby minimizing adsorptive capacity loss. To ensure uniformity of the porous crystal composites with 3dGR thermal additives, the hydrophobicity of 3dGR was controlled by tailoring its surface chemistry. Zeolite (Sigma Aldrich, 13X, 2 μm) was used as the porous adsorbent in this study because it is widely used in various adsorption applications[1, 6, 19-21] and readily available at large quantities. We characterized the adsorption characteristics with water due to its common use in adsorption heat pumps and the high heat of adsorption with many adsorbent materials. The 3dGR-zeolite composites in this study showed a ~200-500% improvement in thermal conductivity over zeolite samples with no additives. Meanwhile, the corresponding decrease in the adsorption capacity was only ~2%. This work provides insights for the development of effective binders to enhance the thermal performance of various porous materials in adsorption systems.

MATERIALS PREPARATION

We used the method of Chen *et al.* to synthesize 3dGR by the template-directed CVD where nickel foam (American Elements, PPI 110) was used as a catalyst.[22] To fabricate the functionalized 3dGR (f3dGR), the surface of the 3dGR was oxidized by a mixture of HNO_3 and H_2SO_4 solutions as described by Menna *et al.*[23] To fabricate the f3dGR-zeolite composite, the zeolite solution (50 wt% zeolite in H_2O) was carefully dropped on top of the wet f3dGR in a beaker. After drying at 105°C for 6 hours, the f3dGR-zeolite composites were pressed at various loading pressures between 10 and 250 MPa to achieve the desired composite density using a 13 mm pellet die (REFLEX Analytical). The corresponding composite density was between 0.607 ± 0.019 and 1.204 ± 0.067 g/cm^3, respectively. Note,

the theoretical density of the zeolite (13X) is ~1.93 g/cm^3.[24] Details for the material preparation can be found in the supporting information.

RESULTS AND DISCUSSION

It is desirable to achieve a uniform mixture of 3dGR and porous crystals to maximize the use of their adsorptive characteristics per given volume. However, despite the advantages of 3dGR (high thermal conductivity, percolated structure and light weight), infiltration hydrophobic 3dGR with adsorptive crystals can be challenging due to the weak surface interaction between the 3dGR and adsorptive crystals. For examples, the synthesized 3dGR in this study was hydrophobic, as shown in the Raman spectra in Figure 1(a). In the black solid line, we observed no disorder (~1340 cm^{-1}, D) mode of 3dGR but the graphite (~1580 cm^{-1}, G) mode before the functionalization. The high G/D intensity ratio (~ 12.3) of the 3dGR confirms infrequent defect sites, resulting in a hydrophobic surface.[25] On the other hand, the adsorption crystals with high adsorption capacity of water are mostly hydrophilic. Therefore, to enhance the surface interaction between the hydrophobic 3dGR and hydrophilic adsorbents, the hydrophilicity of 3dGR was induced by introducing functional groups using a strong acid (HNO_3/H_2SO_4) solution, as described by Menna *et al.*[23] Details of the functionalization can be found in the supporting information. The red solid line in the Raman spectra of Figure 1(a) shows the G and D mode of 3dGR after the functionalization. The intensity of the D mode clearly increased after the functionalization, indicating numerous defect sites on its surface layer.[25] These defect sites have been identified as ideally functionalized-location for the hydroxyl groups on the surface of 3dGR,[26-28] increasing the hydrophilicity. To demonstrate the hydrophilicity of f3dGR, droplet images were captured and the contact angle was measured using a custom MATLAB image analysis code. The droplet angle was defined as the angle measured through the water where the droplet/air interface meets a 3dGR

surface. Figure 1(b) shows the comparison of droplet angles before (3dGR, black circles) and after (f3dGR, red triangles) the functionalization as a function of time. The droplet angle decreased as the droplet penetrated through the f3dGR, while it remained unchanged for the non-functionalized 3dGR with no penetration. Consequently, the zeolite solution (~50 wt% in water) successfully infiltrated with f3dGR while the zeolite solution did not fully penetrate into 3dGR, resulting in a non-uniform composite (Figure S1)

The percolation of 3dGR allows effective phonon transport through its network, resulting in minimizing phonon scattering and a high effective thermal conductivity.[18] Therefore, maintaining the percolation during the fabrication process is important. We found that the percolation was intact even after the infiltration of zeolite particles and the densification of the f3dGR-zeolite composite. We densified the f3dGR-zeolite composites to maximize the adsorption capacity per volume. Figure 2(a) and (b) shows a scanning electron microscope (SEM) images of the f3dGR and the f3dGR-zeolite composite, respectively, confirming its percolated structure before the densification. f3dGR is false-colorized in green for better visual contrast. As shown the red arrow in Figure 2(b), the macropores of f3dGR were filled with zeolites without significant void volume. In addition, as shown by the blue arrow in Figure 2(b), f3dGR was filled with zeolites on the inside, which was beneficial to retain the percolation of f3dGR in the composite even after densification. Furthermore, f3dGR's flexibility can be beneficial to maintain the percolation during densification. Pettes *et al.* demonstrated that 3dGR (< 40 layers) can be flexible.[18] The transmission electron microscopy (TEM) image (Figure 2(c)) indicates that the synthesized f3dGR was composed of approximately 20 - 40 layers of graphene. Consequently, f3dGR (colorized in green) maintained its percolation after the densification, as shown in Figure 2(d). The red and blue arrows in Figure 2(d) show that the zeolites filled in the macropores and the inside of the f3dGR, respectively.

We found that the f3dGR had a significant improvement in the thermal conductivity of the adsorption composite with minimal decrease in its adsorption capacity. Figure 3(a) and 3(b) show a schematic diagram and an experimental setup, respectively, of the variable cold-junction (VCJ) method[29] to measure the thermal conductivity of graphene foams as well as zeolite-graphene foam composites with various densities. Unlike the conventional steady state (SS) method, the VCJ method uses a thermoelectric cooler to cool one end of the sample while keeping the opposite end of the sample at ambient temperature by a resistive heater. Since the heater and the environment were maintained at the same temperature, the heat loss from the heater to the environment through wire conduction and radiation were eliminated. Heat flux through the sample was accurately measured without calibration of the heat loss as in the conventional SS method. We measured the sample thermal conductivity by sweeping across various temperature differences between the TEC cold side and the ambient. The input power to the resistive heater that maintains the opposite side of the sample at the ambient temperature was linearly proportional to the temperature difference across the sample. Since the slope was the thermal conductance of the sample (kA/L, A was the cross-sectional area and L was the thickness of the sample), the thermal conductivity (k) could be determined, as shown in Figure S2.

An annealed f3dGR (Af3dGR) with higher thermal conductivity than that of f3dGR was used for comparison. Annealing the Ni foam at a temperature of 1100 °C before graphene growth increased the grain size by ~2−3 times and created a noticeably smoother surface, resulting in less phonon scattering and a higher thermal conductivity than that of the non-annealed ones.[18] Figure 3(c) shows a comparison between the thermal conductivity of zeolite (black circles), f3dGR-zeolite composite (f3dGR-ZT, red up-triangles) and Af3dGR-zeolite (Af3dGR-ZT, blue down-triangles) for the various composite densities. The thermal conductivity of the zeolite medium increased with density since the overall thermal transport is primarily due to conduction through the solid phase, which is further

enhanced by the increased solid fraction with increased sample density. As shown in Figure 3(c), the thermal conductivity of the f3dGR-zeolite and Af3dGR-zeolite showed a prominent enhancement. The improvements of f3dGR-zeolite and Af3dGR-zeolite compared to that of zeolite were approximately 350% and 500%, respectively, at a low composite density (~0.6 g/cm^3), and approximately 200% and 270%, respectively, at high composite density (~1.2 g/cm^3). The amount of enhancement decreased with densification as the thermal conductivities of the zeolite without the binders increased. Furthermore, the results showed that the relation between the thermal conductivity and density of the composites had good linearity. In fact, Bhattacharya *et al.* also demonstrated this linear increase in thermal conductivity in open-celled metal aluminum foams at low volume fraction (φ).[30]. The empirical relation they derived to calculate the effective thermal conductivity (k_e) of porous metal foam with different media (either water or air) was

$$k_e = \mathrm{A}(\varepsilon k_m + (1-\varepsilon)k_s) + \frac{1-\mathrm{A}}{(\frac{\varepsilon}{k_m}+\frac{1-\varepsilon}{k_s})} \quad (1)$$

where k_e, k_m and k_s represent the effective, medium and solid thermal conductivity, respectively. *A* and ε represent the reported empirical constant and measured porosity, respectively. This empirical relation can be useful in predicting the effective thermal conductivity of f3dGR composites within a porous crystal medium when the thermal conductivities of the f3dGR foam and medium are known individually. In this study, we used the same empirical constant (A = 0.35) as reported by Bhattacharya *et al.* because both studies used an open-celled metal foam structure as a thermal additive. In addition, f3dGR is a percolated few layer graphene which can exhibit a metallic behavior.[31] Zeolite crystals are the medium occupying pores of solid f3dGR. The density and volume fraction (f_{vol}) of the synthesized f3dGR were measured at 0.016±0.001 g/cm^3 and 0.706±0.031%, respectively. We used a dynamic vapor adsorption system (DVS Advantage, Surface Measurement System®) to measure the dry mass of

the f3dGR while minimizing the adsorption of any foreign molecules on its surface. The density was calculated by using the measured dimensions and dried mass. Consequently, the porosity ($\varepsilon = 1 - f_{vol}$) of f3dGR before densification was estimated as 0.9929 ± 0.0003. In order to obtain the thermal conductivity of solid f3dGR (k_s), we used the extreme case of Eq. (1) with vacuum ($k_m = 0$). The f3dGR was the solid frame and the effective thermal conductivity of f3dGR foam (k_f) was measured experimentally by the CB method. We obtained $k_s = \frac{k_f}{0.35(1-\varepsilon)}$, which was very similar to the Lemlich theory originally derived for electronic conductivity and widely applied to thermal conductivity.[32] The k_f of f3dGR and Af3dGR were measured to be 0.14 ± 0.01 and 0.23 ± 0.02 W/mK, respectively. The corresponding k_s of f3dGR and Af3dGR were estimated to be 56.7 and 93.1 W/mK, respectively. The red and blue solid lines in Figure 3(c) show the thermal conductivity trends of f3dGR and Af3dGR, respectively, using the calculated k_s and measured k_m with the empirical model, which demonstrated reasonable agreement with the experimental results. As the composite was pressed, both the thermal conductivity of the medium increase and the decrease of the porosity of the graphene foam resulted in an increased effective thermal conductivity. It is worthwhile to note that the thermal conductivity of 3dGR foam can be higher (0.26~2.28 W/mK) than in this study (0.14~0.23 W/mK) by using a slow nickel etching technique reported by Pettes *et al.*[18] For 3dGR foams with higher thermal conductivity, it is possible to achieve even more dramatic enhancement of the overall thermal conductivity than in this study (see Figure S3) estimated by the empirical relation above.

The percolation of the f3dGR demonstrating effective enhancement in thermal conductivity required only a minimal weight fraction of 3dGR in the composite, resulting in minimal decrease in adsorption capacity. Adsorption capacities were obtained on the DVS Advantage, with which we were able to precisely control vapor pressure and temperature of the small chamber inside. Before adsorption was performed, all absorbents were desorbed. The typical loading mass of absorbent was about 30 mg. The

errors in the measurements were minimal due to the exceptional sensitivity (0.1 μg) of the DVS Advantage. Figure 3(d) shows that both f3dGR-zeolite and Af3dGR-zeolite composites had minimal reduction in adsorption capacity (~2%) due to their minimal weight contribution. In addition, Figure S4 shows XRD patterns of zeolite without (black) and with f3dGR (red). There was no significant loss of crystallinity even after the zeolite infiltration with f3dGR. Because the zeolite micropores remained intact after the filtration, the composite showed no significant reduction of adsorption, as shown in Figure 3(d). Therefore, unlike conventional thermal additives, such as carbon nanotubes, graphene and graphite, distinct advantages of the f3dGR are the effective enhancement in thermal conductivity due to its percolated structure and the minimal reduction of adsorption capacity due to the light weight and small volume fraction of f3dGR.

CONCLUSION

We demonstrated f3dGR to be a promising thermal additive to effectively increase thermal conductivity in a porous crystal adsorption bed. We showed an enhanced thermal conductivity of the adsorption composite, up to ~500%, at a low zeolite packing density of ~0.6 g/cm^3 using f3dGR as a thermal additive while minimizing the decrease of vapor-uptake to only ~2% due to their minimal weight contribution. The functionalization was found to be an effective way to implement a hydrophobic carbon network with porous crystals regardless of its hydrophobicity. f3dGR can be applicable to numerous types of porous crystals, including metal organic frameworks, to overcome the drawback of low thermal conductivity. Our findings are beneficial to realizing various adsorption systems, such as thermal adsorptive storage, heat pumps, chillers, hydrogen adsorption and carbon dioxide adsorption systems. However, for f3dGR to become a practical solution as an effective thermal

additive for adsorptive porous crystals, future work should focus on synthesizing f3dGR using more cost-effective metals and developing flexible carbon network with low cost.

ACKNOWLEDGMENT

This work is supported by ARPA-E with Dr. James Klausner and Dr. Ravi Prasher as program managers.

REFERENCES

[1] S. Narayanan, S. Yang, H. Kim, E.N. Wang. Int. J. Heat Mass Transfer **77**, 288 (2014)
[2] J. Zhang, P.V. Ramachandran, J.P. Gore, I. Mudawar, T.S. Fisher. J. Heat Transfer **127** (12), 1391 (2005)
[3] Y. Liu, Z.U. Wang, H.-C. Zhou. Greenhouse Gases Sci. Technol. **2**(4), 239 (2012)
[4] H. Furukawa, F. Gándara, Y.-B. Zhang, J. Jiang, W.L. Queen, M.R. Hudson, O.M. Yaghi. J. Am. Chem. Soc. **136**(11), 4369 (2014)
[5] J. Weitkamp, M. Fritz, S. Ernst. Int. J. Hydrogen Energy **20**(12), 967 (1995)
[6] S. Narayanan, X. Li, S. Yang, H. Kim, A. Umans, I.S. McKay, E.N. Wang. Appl. Energy **149**, 104 (2015)
[7] F. Jeremias, D. Fröhlich, C. Janiak, S.K. Henninger. New J. Chem. **38**(5), 1846 (2014)
[8] J.A. Greathouse, M.D. Allendorf. J. Am. Chem. Soc. **128**(33), 10678 (2006)
[9] E. Poirier, A. Dailly. Nanotechnology **20**, 204006 (2009).
[10] K.C. Chan, C.Y.H. Chao, M. Bahrami. Heat and Mass Transfer Characteristics of a Zeolite 13X/CaCl2 Composite Adsorbent in Adsorption Cooling Systems. 49-58 (2012) http://repository.ust.hk/ir/Record/1783.1-56148
[11] V. Colombo, S. Galli, H.J. Choi, G.D. Han, A. Maspero, G. Palmisano, N. Masciocchi, J.R. Long. Chem. Sci. **2**(7), 1311 (2011)
[12] S. Yang, H. Kim, S. Narayanan, I.S. McKay, E.N. Wang. Mater. Des. **85**, 520 (2015)
[13] L. Pino, Y. Aristov, G. Cacciola, G. Restuccia. Adsorption **3**(1), 33 (1997)
[14] J. Purewal, D. Liu, A. Sudik, M. Veenstra, J. Yang, S. Maurer, U. Müller, D.J. Siegel. J. Phys. Chem. C **116**(38), 20199 (2012)
[15] Y. Ming, J. Purewal, D.a. Liu, A. Sudik, C. Xu, J. Yang, M. Veenstra, K. Rhodes, R. Soltis, J. Warner, M. Gaab, U. Müller, D.J. Siegel. Microporous Mesoporous Mater. **185**, 235 (2014)
[16] M. Zhou, H. Bi, T. Lin, X. Lü, F. Huang, J. Lin. J. Mater. Chem. **A 2**(7), 2187 (2014)
[17] M. Zhou, H. Bi, T. Lin, X. Lü, D. Wan, F. Huang, J. Lin. Carbon **75**, 314 (2014)
[18] M.T. Pettes, H. Ji, R.S. Ruoff, L. Shi. Nano Lett. **12**(6), 2959 (2012)
[19] X. Li, S. Narayanan, V.K. Michaelis, T.-C. Ong, E.G. Keeler, H. Kim, I.S. McKay, R.G. Griffin, E.N. Wang. Microporous Mesoporous Mater. **201**, 151 (2015)
[20] J. Jänchen, D. Ackermann, H. Stach, W. Brösicke. Sol. Energy **76**(1–3), 339 (2004)
[21] H. Demir, M. Mobedi, S. Ülkü. **12**(9), 2381 (2008)
[22] Z. Chen, W. Ren, L. Gao, B. Liu, S. Pei, H.-M. Cheng. Nat. Mater. **10**(6) 424 (2011)
[23] E. Menna, F. Della Negra, M. Dalla Fontana, M. Meneghetti. Phys. Rev. B **68**(19), 193412 (2003)
[24] D. Novembre, B. Di Sabatino, D. Gimeno, M. Garcia-Vallès, S. Martínez-Manent. Microporous Mesoporous Mater. **75**(1–2), 1 (2004)
[25] A.C. Ferrari, J. Robertson. Phys. Rev. B **61**(20), 14095 (2000)
[26] K. Chen, S. Song, F. Liu, D. Xue. Chem. Soc. Rev. **44**(17), 6230 (2015)
[27] K. Chen, S. Song, D. Xue. J. Mater. Chem. A **3**(6), 2441 (2015)
[28] F. Liu, D. Xue. Chem. Eur. J. **19**(32), 10716 (2013)
[29] D. Kraemer, G. Chen. Rev. Sci. Instrum. **85**(2), 025108 (2014)
[30] A. Bhattacharya, V.V. Calmidi, R.L. Mahajan. **45**(5), 1017 (2002)
[31] S. Latil, L. Henrard. Phys. Rev. Lett. **97**(3), 036803 (2006)
[32] R. Lemlich. J. Colloid Interface Sci. **64**(1), 107 (1978)

FIGURE CAPTIONS

Figure 1: (a) Raman spectra of 3dGR (black solid) and f3dGR (red solid). (b) Comparison of droplet angle between 3dGR (black circles) and f3dGR (red triangle) as a function of time. The water droplets on 3dGR (right-top) and f3dGR (right-bottom) were captured 20 seconds after release onto the surfaces.

Figure 2: SEM images of (a) f3dGR and (b) f3dGR-zeolite composite showing its percolated structure. f3dGR was false-colorized in green for better contrast and zeolite particles are shown in grey. (c) A TEM image of f3dGR composed of multiple layers of graphene. (d) A SEM image of f3dGR-zeolite composite after densification at ~ 100 MPa.

Figure 3: (a) Schematic diagram and (b) experimental set-up of the VCJ method. (c) Thermal conductivity comparisons of zeolite (black circle), f3dGR-zeolite (f3dGR-ZT, red up-triangle) and Af3dGR-zeolite (Af3dGR-ZT, blue down-triangle). Solid lines are from modeling with f3dGR (red solid) and Af3dGR (blue solid) foams with thermal conductivity of 0.14 W/mK and 0.23 W/mK, respectively. (d) Adsorption capacity comparison of zeolite (black circle), f3dGR-ZT (red up-triangle) and f3dGR-ZT (blue down-triangle).

FIGURE

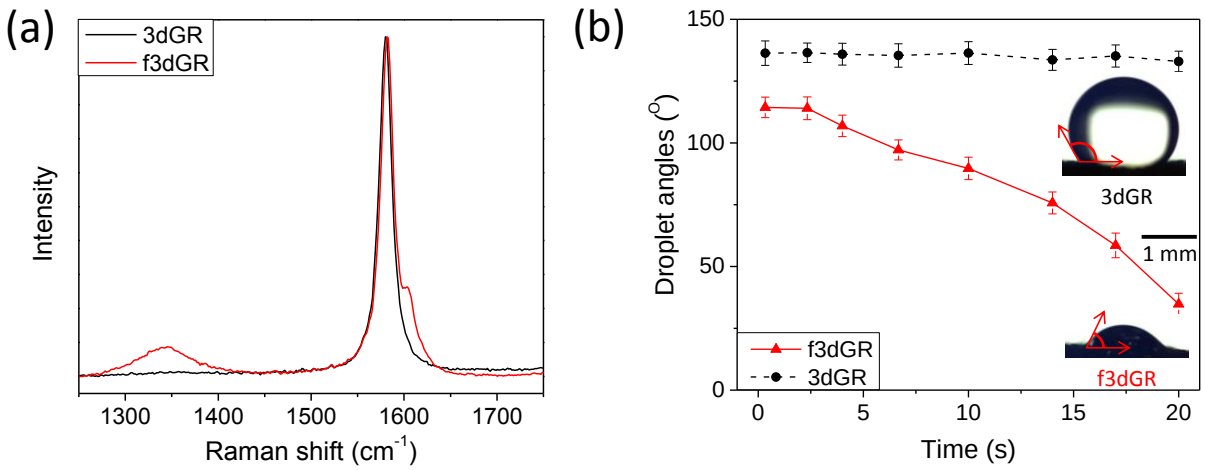

Figure 1: (a) Raman spectra of 3dGR (black solid) and f3dGR (red solid). (b) Comparison of droplet angle between 3dGR (black circles) and f3dGR (red triangle) as a function of time. The water droplets on 3dGR (right-top) and f3dGR (right-bottom) were captured 20 seconds after release onto the surfaces.

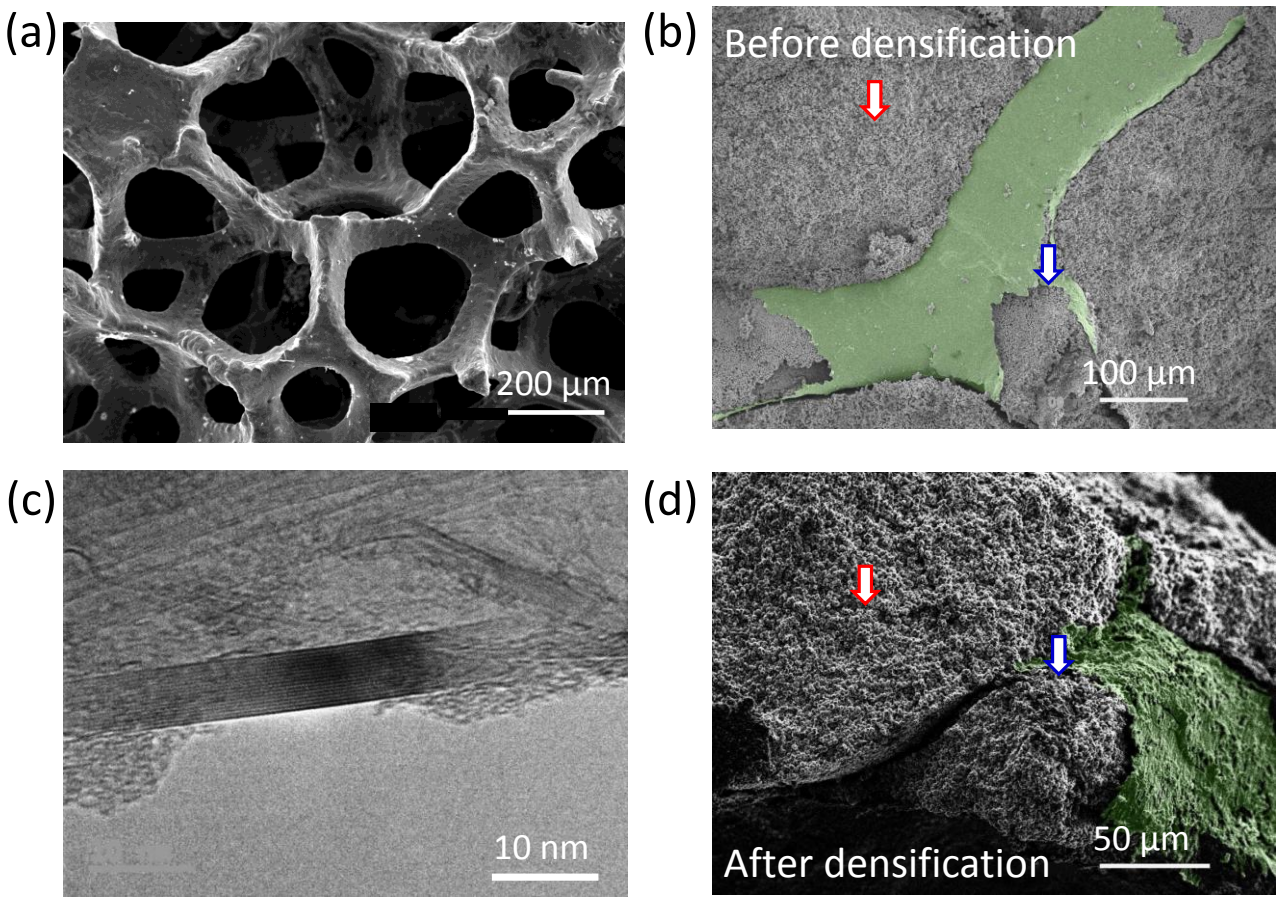

Figure 2: SEM images of (a) f3dGR and (b) f3dGR-zeolite composite showing its percolated structure. f3dGR was false-colorized in green for better contrast and zeolite particles are shown in grey. (c) A TEM image of f3dGR composed of multiple layers of graphene. (d) A SEM image of f3dGR-zeolite composite after densification at ~ 100 MPa.

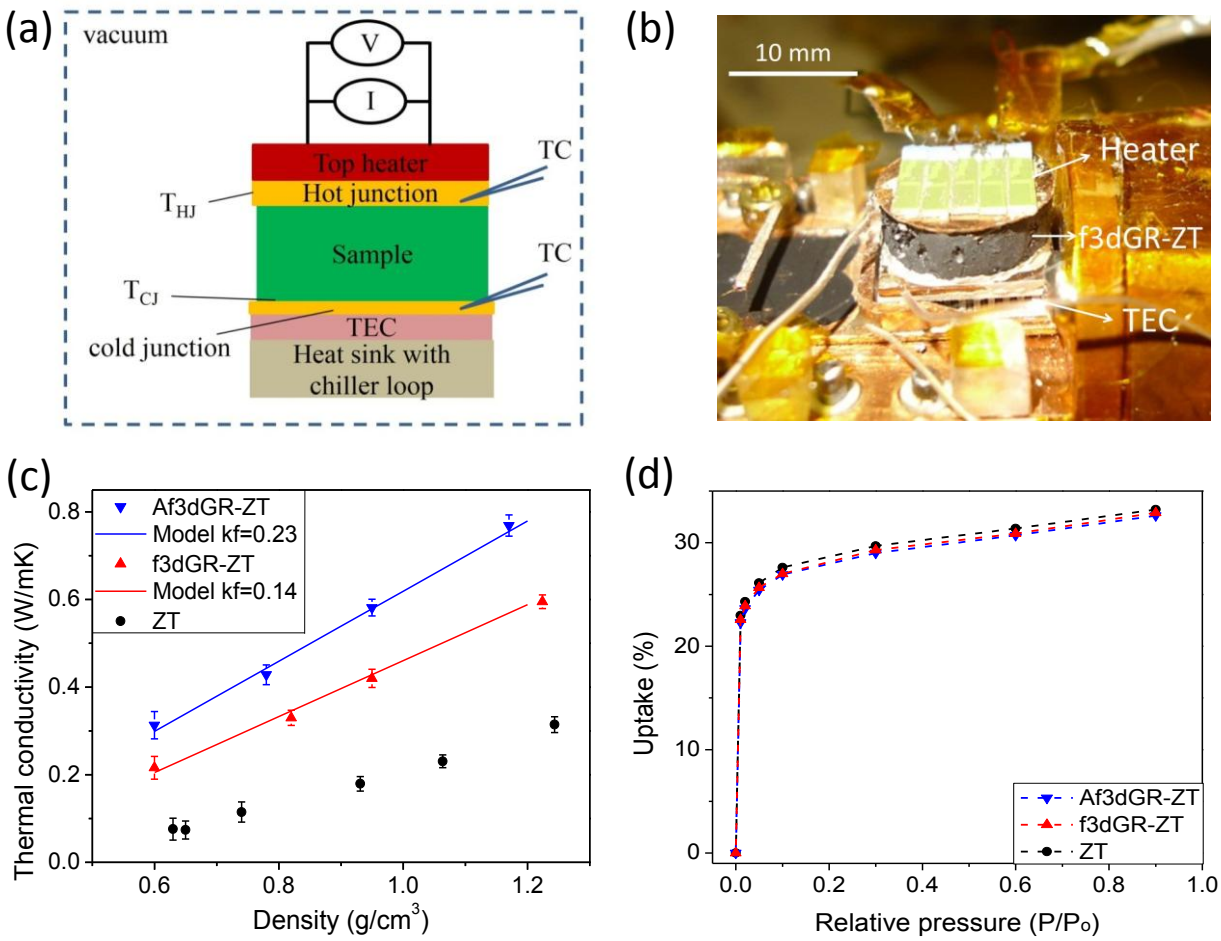

Figure 3: (a) Schematic diagram and (b) experimental set-up of the VCJ method. (c) Thermal conductivity comparisons of zeolite (black circle), f3dGR-zeolite (f3dGR-ZT, red up-triangle) and Af3dGR-zeolite (Af3dGR-ZT, blue down-triangle). Solid lines are from modeling with f3dGR (red solid) and Af3dGR (blue solid) foams with thermal conductivity of 0.14 W/mK and 0.23 W/mK, respectively. (d) Adsorption capacity comparison of zeolite (black circle), f3dGR-ZT (red up-triangle) and f3dGR-ZT (blue down-triangle).

SUPPORTING INFORMAITON

Synthesis of 3dGR: We used the method of Chen *et al.* to synthesize 3dGR by the template-directed CVD where nickel foam (American Elements, PPI 110) was used as a catalyst.[22] Methane, hydrogen and argon gases (CH_4, H_2 and Ar) were used for growth. For the pre-annealing process, Ni foam was annealed for about 24 hours at 1100 ºC under flowing H_2 (40 sccm) and cooled down to room temperature at 0.5 ºC/min before conducting CVD growth to enlarge Ni grain size resulting in higher thermal conductivity of 3dGR than that without the pre-annealing process. The Ni foam was cut into desired size strips, followed by placing them in a furnace (Lindburg BlueM®). The temperature of the furnace was ramped to 1000 ºC in 1 hour under flowing Ar (40 sccm) and H_2 (10 sccm) mixture and held for an additional 30 minutes. To coat graphene on Ni foam, the mixture of CH_4 (50 sccm), H_2 (50 sccm) and Ar (400 sccm) was introduced for 1 hour at 1000 ºC. After the growth, the furnace was quickly cooled down to room temperature (20 ºC min^{-1}). After the growth of 3dGR on nickel foam, the nickel foam was etched by placing the sample in a diluted HCl acid solution for 3 days at 50˚C.

Synthesis of f3dGR-zeolite composite: The surface of the synthesized 3dGR was selectively functionalized by the mixture of HNO_3 and H_2SO_4 solution. The HCl wetted 3dGR was washed with fresh water multiple times until its pH became neutral. The washed 3dGR was then placed in two diluted HNO_3 acids (10 wt%, followed by 20 wt%) to avoid the rigorous reaction between HNO_3 and the water, which can result in damage of the 3dGR. The acid wetted 3dGR was finally placed in the acid mixture of HNO_3 and H_2SO_4 (3:1 volume ratio) for the functionalization at 70 ºC for 1 hour. After functionalization, 3dGR was taken out and placed in a 10% diluted HNO_3 acid solution, followed by washing with fresh water. Due to surface tension, drying f3dGR often resulted in collapsing the foam structure of f3dGR. Therefore, the synthesized f3dGR was kept in water before the infiltration of zeolite particles. A wet f3dGR was placed in a beaker, and the zeolite solution (50 wt%) was carefully dropped on top of the wet f3dGR. After 6 hours, zeolite particles settled down in the bottom of the beaker,

separated from the bulk of the water. After decanting the water on the top, the f3dGR- zeolite composites were dried in an oven at 105°C for 6 hours and then excess zeolites were carefully removed from the f3dGR- zeolite composites by using a blade. The synthesized f3dGR- zeolite composites were pressed at various loading pressure between 10 and 250 MPa to achieve a desired composite density using a 13 mm pellet die (REFLEX Analytical). The corresponding composite densities varied between 0.607 ± 0.019 and 1.204 ± 0.067 g/cm^3, respectively.

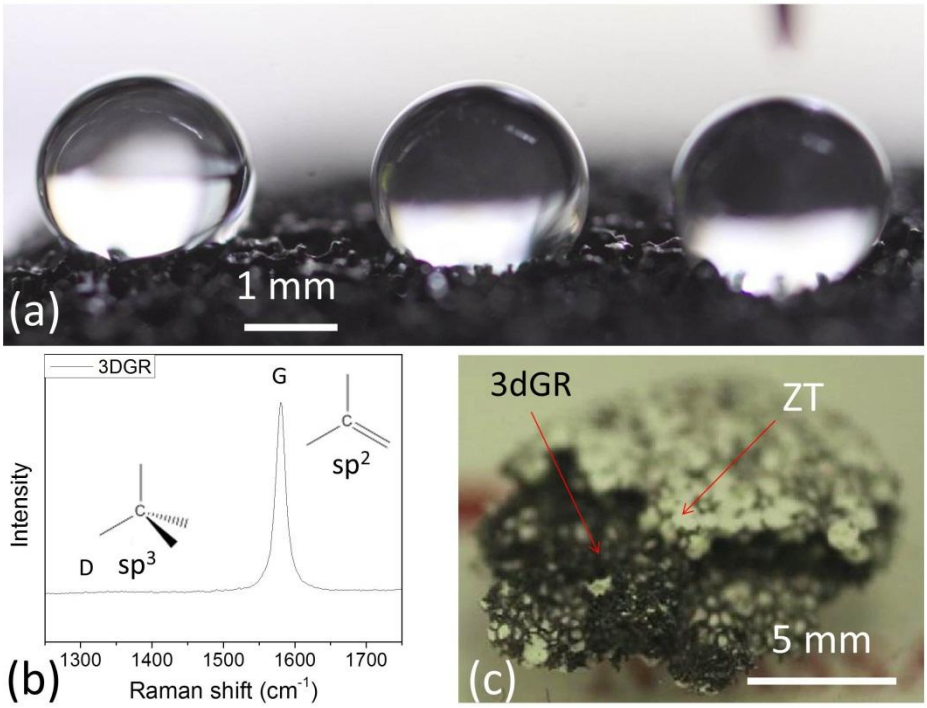

Figure S1: (a) Droplets resting on top of the 3dGR (non-functionalized 3dGR), which do not penetrate through. (b) Raman spectra of 3dGR showing high G/D ratio indicating minimal defect sites. (c) Image showing a 3dGR-zeolite composite indicating its non-uniformity.

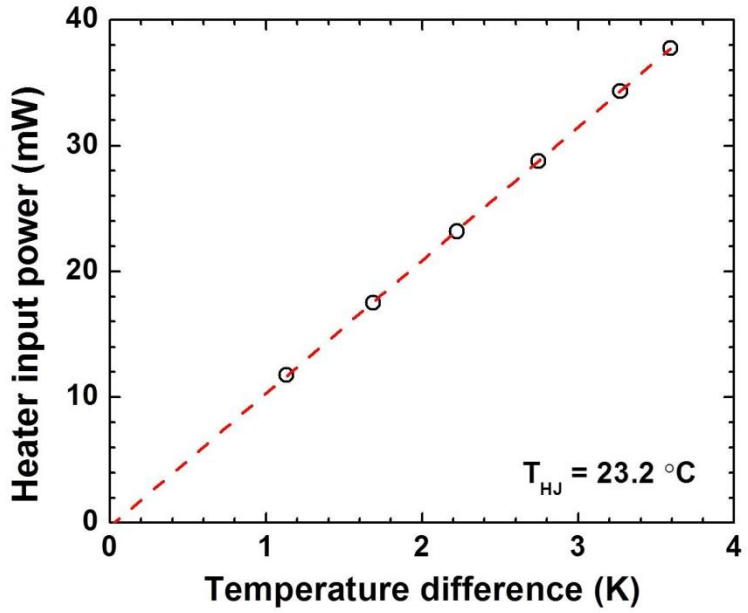

Figure S2: Typical temperature difference responses to various heater input powers using the VCJ method. Thermal conductivity (k) of Af3dGR was calculated at 0.34 W/mK. The temperature of the hot junction (T_{HJ}) was 23.2 °C.

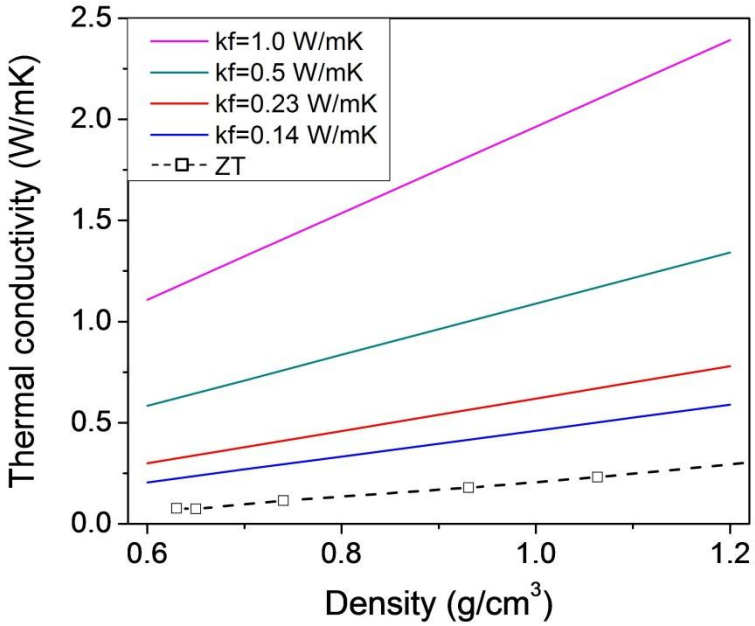

Figure S3: Predictions of effective thermal conductivity of f3dGR-zeolite composites using the empirical relation, equation (1), varying the thermal conductivity of the 3dGR foam (0.14, 0.23, 0.5 and 1.0 W/mK).

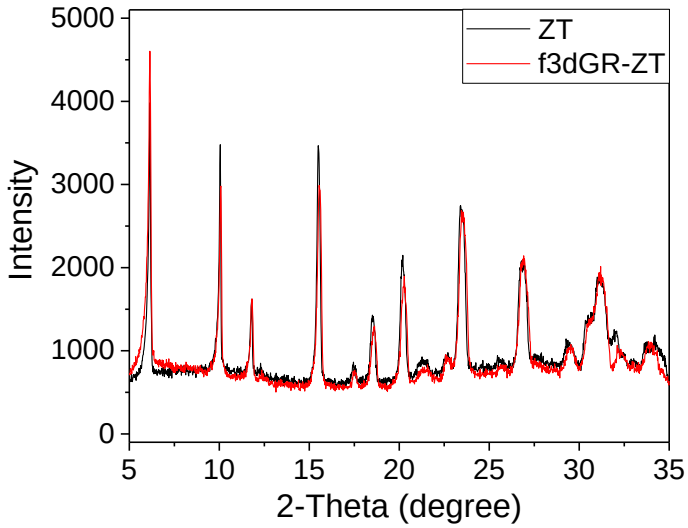

Figure S4: XRD patterns of zeolite (ZT) without (black) and with f3dGR (red) showing that there was no significant loss of crystallinity even after the zeolite infiltration with f3dGR. Because the zeolite micropores remained intact after the filtration, the composite showed no significant reduction in adsorption.